Journal of Materials Chemistry

Cite this: *J. Mater. Chem.*, 2011, **21**, 6975

www.rsc.org/materials

PAPER

Synthesis and electrochemical properties of $LiFePO_4$/C composite cathode material prepared by a new route using supercritical carbon dioxide as a solvent

Jingwen Zhang,[ab] Linhai Zhuo,[a] Leilei Zhang,[ab] Chaoyong Wu,[ab] Xinbo Zhang*[a] and Limin Wang*[a]

Received 12th January 2011, Accepted 8th March 2011
DOI: 10.1039/c1jm10168d

From the viewpoint of energy efficiency and cost, an intensive search for less energy demanding synthesis methods for $LiFePO_4$ appears quite attractive and is still in full swing. Here, we report that carbon coated $LiFePO_4$ ($LiFePO_4$/C) powders can be successfully synthesized by a new route using supercritical carbon dioxide as a solvent. The obtained high-purity $LiFePO_4$/C powders are uniform in shape and 0.5 μm to 1 μm in size. As for the electrochemical performance, at the current density of 0.1 C, the electrode exhibits a discharge capacity of 158 mA h g^{-1} as well as good cycling stability—there is no obvious capacity fading after 100 cycles. When the synthesis reaction temperature increases from 50 to 200 °C, the primary particle size grows from approximately 0.5 to 2 μm, and the initial discharge capacity decreases from 158 to 41 mA h g^{-1}, which shows that 50 °C is the optimum temperature to synthesize $LiFePO_4$ in supercritical carbon dioxide. Needless to say, such a new approach, which is not specific to $LiFePO_4$, offers great opportunities for the synthesis of new electrode materials.

Introduction

Energy storage by rechargeable batteries has become an issue of strategic importance as it will play a critical role in clean energy generation and use.[1] Among all advanced battery systems, the lithium-ion battery has taken less than 20 years to successfully capture the portable electronic market, thanks to its attractive energy density and cycle-life performance.[2] However, when it is proposed to conquer the upcoming markets of electric transportation (*e.g.*, hybrid electric vehicles) and renewable energies (*e.g.*, wind or solar energy), great improvements are urgently needed, with the top of the list being safety and cost of cell components (anodes, electrolytes, or cathodes).[3] As for the cathode, besides right voltage (3.45 V *vs.* Li^+/Li) and high specific capacity (170 mA h g^{-1}), inherently high safety has rendered olivine-type $LiFePO_4$ of great interest as a promising cathode material for Li-ion batteries when used for electric vehicles or larger-scale power systems.[4]

Up to now, the most common and traditional method to manufacture $LiFePO_4$ is still high-temperature ceramic routes, which include grinding, ball milling and heat treatment at 300–800 °C.[5] Alternatively, some other methods reported are high cost and impractical for using expensive Fe(II) materials and complicated synthesis techniques.[6] From the viewpoint of energy efficiency and cost, besides addressing fundamental aspects regarding the influence of particle size/defect,[7–11] cationic/anionic substitute[12,13] or surface coating[14–20] on insertion/deinsertion mechanism and capacity/rate performances of $LiFePO_4$, a great amount of work is presently aimed at new low-cost processes to make highly electrochemically optimized $LiFePO_4$ powders.[21–25] From this context, low-temperature hydro(solvo)thermal processes have received increased attention with successful results. Most recently, Tarascon *et al.* reported a new eco-efficient ionothermal synthetic approach for tailor-made $LiFePO_4$ powders.[26] Regardless of the specificity of the hydro(solvo) thermal approach, the carbon-coating of the resulting powders is always beneficial to their electrochemical performances.

The intensive search for alternative low-temperature syntheses of $LiFePO_4$ appears quite attractive and is in full swing. Supercritical carbon dioxide ($scCO_2$) refers to carbon dioxide that is in a fluid state while also being at or above both its critical temperature (31.1 °C) and pressure (7.39 MPa). It is an attractive alternative to conventional organic solvents due to its unique features of tunable physical properties and environmental benignness.[27] Carbon dioxide is inexpensive, environmentally benign, and non-flammable with low viscosity, "zero" surface tension, and high diffusivity in its supercritical condition, that is favorable for synthesizing superior ultrafine and uniform nanomaterials.[27] Over the past decade, $scCO_2$ synthesis has been developed into an advantageous synthetic technique for organic

[a]*State Key Laboratory of Rare Earth Resource Utilizations, Changchun Institute of Applied Chemistry, Chinese Academy of Sciences, 5625 Renmin Street, Changchun, China 130022. E-mail: xbzhang@ciac.jl.cn; lmwang@ciac.jl.cn*
[b]*Graduate School of the Chinese Academy of Sciences, Beijing, China 100039*

synthesis,[27] especially in catalytic hydrogenation, hydroformylation, free radical reaction, oxidation reaction, Friedel–Crafts alkylation and enzymatic catalytic reaction, but to the best of our knowledge, there have not been any reports on the synthesis of $LiFePO_4$ *via* $scCO_2$. In this work, we describe a facile synthesis method for carbon coated $LiFePO_4$ ($LiFePO_4$/C) with a well defined shape and uniform particle size, wherein $scCO_2$ is used as a solvent and low-cost $Fe(NO_3)_3 \cdot 9H_2O$ as a precursor. The obtained $LiFePO_4$/C exhibits a high capacity and a good cycling stability without obvious capacity fading up to 100 cycles. For comparison and elucidation of the efficiency of $scCO_2$, absolute ethanol and a mixture of absolute ethanol and $scCO_2$ are also employed as a solvent. In addition, we also change the reaction temperatures to alter the property of $scCO_2$ solvent and thus adjust the morphology and electrochemical performance of the synthesized material.

Experimental section

All chemicals were used as received without further purification. Lithium nitrate ($LiNO_3$), ferric nitrate ($Fe(NO_3)_3 \cdot 9H_2O$), ammonium phosphate monobasic ($NH_4H_2PO_4$) and sucrose ($C_{12}H_{22}O_{11}$) were all purchased from Beijing Chemical Works.

Different samples (a, b, and c) of $LiFePO_4$/C were prepared in different solvents: (a) in absolute ethanol, (b) in a mixture of absolute ethanol and $scCO_2$, and (c) in $scCO_2$. In a typical process, $LiNO_3$, $Fe(NO_3)_3 \cdot 9H_2O$, $NH_4H_2PO_4$ and $C_{12}H_{22}O_{11}$ with a molar ratio of 1 : 1 : 1 : 0.5 were placed in three Teflon-lined stainless steel autoclaves, and 10 ml absolute ethanol was added separately into (a) and (b). Liquid CO_2 was compressed into (b) and (c) using a high-pressure liquid pump to 10 MPa, and then (a), (b) and (c) were kept constant and stirred at 50 °C for 10 h. The obtained slurry should be dried in air (removing the water in the reactants to prevent segregation) and completely ground to fine powders. Then they were translated to and kept in autoclaves again using the same procedure described above except the time was prolonged to 24 h at 50 °C. For comparison, we also prepared samples at a range of temperatures (100, 150 and 200 °C). The resulting powders were annealed at 350 °C for 5 h (heating rate of 5 °C min^{-1}) under a mixed atmosphere of N_2 (95%) and H_2 (5%). The obtained powder was slightly ground and then sintered at 600 °C for 10 h in the mixed atmosphere.

Powder X-ray diffraction (XRD) was performed on a Rigaku D/MAX-2500 diffractometer. The morphology of the materials was analyzed by the scanning electron microscope (SEM Hitachi S-4800). Transmission electron microscope (TEM) and selected area electron diffraction (SAED) were recorded on a Tecnai G20 operating at 200 kV for the detailed microstructure information of the sample. X-Ray photoelectron spectroscopy (XPS) was recorded on an ESCALAB 250 spectrometer. The monochromatized Al Kα X-ray source was operated at 12 kV and 20 mA. Analysis of the XPS spectra was done using XPS Peak-fit software. The electronic conductivity of $LiFePO_4$/C powders synthesized by $scCO_2$ at different temperatures was measured with a four-point probe.

The cathode consisted of 80 wt% $LiFePO_4$/C material, 10 wt% poly(vinylidene fluoride) as a binder, and 10 wt% acetylene black as a conducting agent. After being blended in *N*-methyl-pyrrolidinone, then the slurry was spread uniformly on aluminium foil and dried at 120 °C for 12 h in vacuum. A typical cathode disk contained active material of 6–8 mg cm^{-2}. Charge and discharge performances of the electrodes were evaluated using 2025 coin cells containing an electrolyte solution of 1 M $LiPF_6$ in a mixed solvent of ethylene carbonate and dimethyl carbonate (1 : 1 volume ratio) in a Celgard2320 micro-porous separator membrane. Lithium foil served as the counter electrode. The cells were assembled in an argon-filled glove box (O_2 and H_2O levels <1 ppm). The galvanostatic charge and discharge were controlled between 2.5 and 4.2 V on a LAND CT2001 A cell test instrument (Wuhan Kingnuo Electronic Co., China).

Results and discussion

Illustrated in Fig. 1 are the typical XRD patterns of the products prepared with different solvents. All the patterns can be identified to be an orthorhombic olivine structure with a space group of *Pnmb*. No impurities such as Li_3PO_4 and others, which often appear in the $LiFePO_4$ product synthesized by traditional routes, are observed. No obvious peaks corresponding to graphite are found in the XRD pattern, indicating that the carbon in the sample is not well crystallized.[28] It should be noted that the diffraction peaks of sample (c) are slightly sharper than those of (a) and (b). This indicates that the crystallinity of sample (c) is better than those of others (samples (a) and (b)), which might be due to the big difference in polarity of the solvent with different compositions of ethanol (polar) and $scCO_2$ (non-polar).

To further confirm the successful synthesis of the $LiFePO_4$/C composite, X-ray photoelectron spectroscopy, as a non-destructive technique and well-suited for evaluation of valence states of metal/non-metal ions and extensively used in the characterization of cathode materials,[29,30] is employed. The typical core level spectra for Li 1s, Fe 2p, P 2p and O 1s for sample (c) are shown in Fig. 2. It can be seen that Li 1s is centered at approximately 55.35 eV (Fig. 2a), which matches well with the binding energy (BE) of Li^+ in $LiFePO_4$ and layered cathode materials.[29] The Fe $2p_{3/2}$ and $2p_{1/2}$ peaks in the compound (Fig. 2b) show BE of 710.8 and 724.6 eV, respectively, which are in good agreement with values reported for $LiFePO_4$.[30,31] The single peak (Fig. 2c) for P 2p shows a BE of 133.35 eV, which is characteristic of the tetrahedral PO_4 group. The O 1s peak with a BE of 531.31eV can

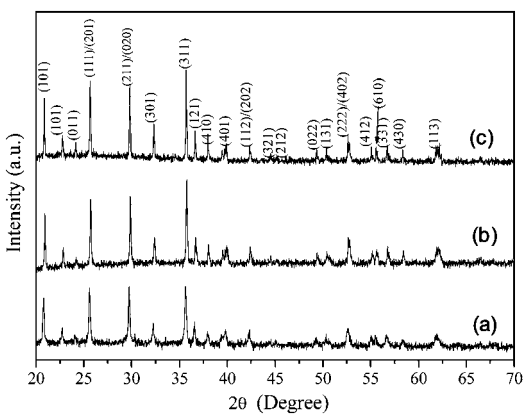

Fig. 1 XRD patterns of the samples synthesized with absolute ethanol (a), with a mixture of absolute ethanol and $scCO_2$ (b), and with $scCO_2$ (c).

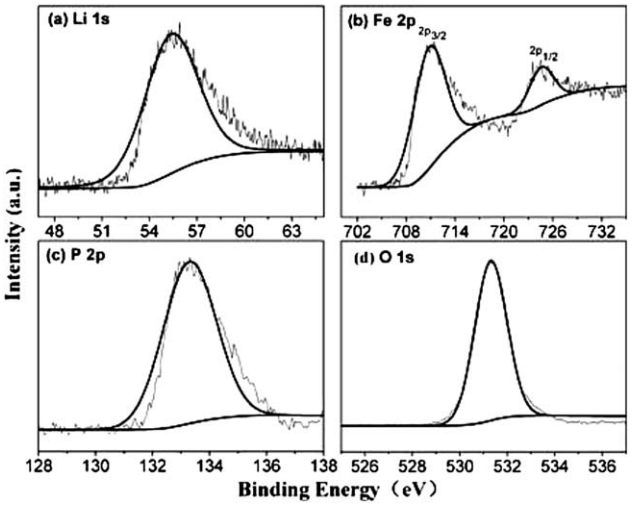

Fig. 2 X-Ray photoelectron spectra (XPS) of the $LiFePO_4$/C particles (sample (c)) synthesized with $scCO_2$.

be assigned to oxygen predominantly bonded to Fe ions in the lattice.

Fig. 3 shows SEM images of $LiFePO_4$/C prepared in different solvents. It can be easily seen that the solvents have a significant influence on the morphology of the prepared samples. In the case of absolute ethanol (Fig. 3a), the particle size is in the range of 0.2–2 μm and not uniform. When the solvent is changed to a mixture of absolute ethanol and $scCO_2$, the primary particle size becomes smaller and falls into the range of 0.4–1 μm (Fig. 3b). Interestingly, the size and morphology of the products prepared in $scCO_2$ are presented in Fig. 3c, which suggests that the diameter of $LiFePO_4$/C is reduced obviously and the typical size is in the range of 0.5 μm to 1 μm. These results clearly show that the solvents play a crucial role in the size and morphology of $LiFePO_4$/C. This might also be related to the big difference in polarity between $scCO_2$ and ethanol. The solubility of the product in non-polar $scCO_2$ is lower than that in polar ethanol. That is to say, the supersaturation of the product in $scCO_2$ is higher than that in ethanol. This could affect the nucleation and/or growth of the product and, as a result, higher supersaturation would lead to the formation of smaller particles[32,33] and *vice versa*.[34] The fact that relatively small and uniform particles can only be obtained in the existence of $scCO_2$ indicates the importance of $scCO_2$ in the formation of $LiFePO_4$/C particles. In addition, the energy-dispersive X-ray (EDX) spectra (Fig. 3d) confirm the co-existence of Fe, P, O and C elements in the prepared sample again, which is consistent with the result of XPS.

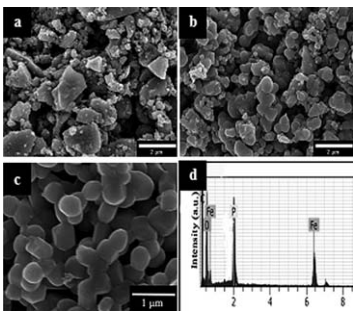

Fig. 3 Scanning electron microscopy (SEM) images of $LiFePO_4$/C prepared under different conditions: (a) absolute ethanol, (b) a mixture of absolute ethanol and $scCO_2$, (c) $scCO_2$, and (d) energy-dispersive X-ray (EDX) spectra of $LiFePO_4$/C prepared under $scCO_2$.

In order to further investigate the microstructure and confirm the carbon distribution and crystallinity of the as-synthesized materials, we have applied TEM and SAED on the prepared sample. As seen in Fig. 4a, the surface of $LiFePO_4$ is coated with a carbon layer of less than 20 nm in thickness, which is thought to be favourable for electronic inter-particles connection, but would not block the direct contact between the active particles and the penetrated electrolyte. In addition, in the high-resolution TEM (HRTEM) image (Fig. 4b), clear lattice fringes can be found in the core area but not in the surface, indicating that the surface carbon is in an amorphous state. The width (0.428 nm) of neighbouring lattice fringes corresponds to the (101) plane of $LiFePO_4$. The related SAED pattern (Fig. 4c) exhibits a regular and clear diffraction spot array, which indicates that the particle is single-crystalline and can be indexed as the $LiFePO_4$ orthorhombic phase. These results are in good agreement with the results of XRD and XPS, further confirming the successful synthesis of crystallized $LiFePO_4$ coated with amorphous carbon.

To test the electrochemical performance of the prepared $LiFePO_4$/C, coin cells using a $LiFePO_4$/C cathode and lithium anode are charged and discharged between 2.5 and 4.2 V. Fig. 5 displays the initial charge/discharge voltage profiles of the $LiFePO_4$/C synthesized in different solvents. It can be found that all the cells exhibit one charge and discharge plateau around 3.4 V, which reflects that the process of lithium deposition and dissolution is smooth in every case. As for the discharge capacity, interestingly, the electrode containing $LiFePO_4$/C synthesized in $scCO_2$ (sample (c)) exhibits a discharge capacity of 158 mA h g^{-1} at a current rate of 0.1 C, which is close to the theoretical capacity of 170 mA h g^{-1} and much higher than those of $LiFePO_4$/C prepared in other solvents (47 and 92 mA h g^{-1} for sample (a) and sample (b), respectively). Moreover, the coulombic efficiency (the ratio of charge capacity to discharge capacity) for sample (c) is >98% indicating a good reversibility, which is much higher than those of the latter two samples (83% for sample (a) and 73% for sample (b)). The smaller particle size of sample (c) may contribute to the better charge and discharge capabilities, which may arise from the enhanced contact area between the $LiFePO_4$/C cathode and the electrolytes.

Fig. 6 shows a plot of discharge capacity *vs.* cycle number of the $LiFePO_4$/C at 0.1 C and 1 C rates. As can be seen, in the case

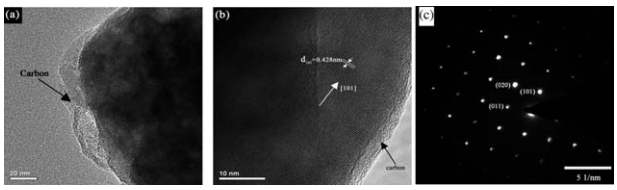

Fig. 4 (a) Transmission electron microscopy (TEM) image of $LiFePO_4$/C (sample (c)) prepared in $scCO_2$, (b) high-resolution TEM image, and (c) the selected area electron diffraction (SAED) pattern.

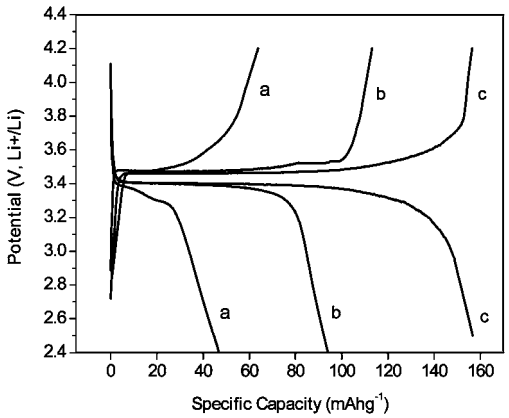

Fig. 5 The initial charge/discharge profiles of sample (a) (synthesized in absolute ethanol), sample (b) (synthesized in a mixture of absolute ethanol and $scCO_2$) and sample (c) (synthesized in $scCO_2$) at a current rate of 0.1 C.

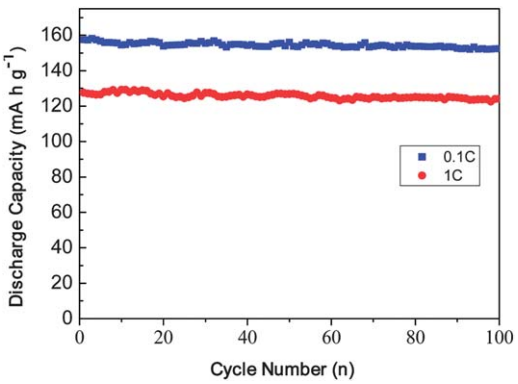

Fig. 6 Discharge capacity *vs.* cycle number of $LiFePO_4$/C (sample (c)) synthesized with $scCO_2$ at 0.1 C and 1 C charge/discharge rates between 2.5 and 4.2 V.

of 0.1 C, although the discharge capacity monotonously decreases from 158 to 150 mA h g^{-1} during the first 10 cycles, it then fluctuates between 152 and 159 mA h g^{-1} during the successive cycles. Interestingly, while the initial discharge capacity is only 128 mA h g^{-1} at 1 C, there is no obvious capacity fading even after 100 cycles. These results demonstrate the well cycling stability of the $LiFePO_4$/C prepared in $scCO_2$.

Charge and discharge profiles obtained from coin-type cells containing $LiFePO_4$/C cathodes with increasing *C* rates from 0.1 to 2 C between 2.5 and 4.2 V are presented in Fig. 7. It can be seen that the discharge capacity decreases with the increase of current rate. At the rate of 2 C, the discharge capacity is 96 mA h g^{-1}, corresponding to a capacity retention of 61% (compared with the capacity at a rate of 0.1 C). It should be noted that full recovery of the capacity can be obtained when the *C* rate is decreased to 0.1 C, indicating that the electrode and the formed solid electrolyte interface (SEI) are stable during the cycles. The relatively poor discharge performance of our synthesized $LiFePO_4$/C at high rates reminds us that the low electronic conductivity and slow lithium-ion diffusion coefficient, which are the intrinsic problems of $LiFePO_4$ materials, should be further improved in our future efforts.

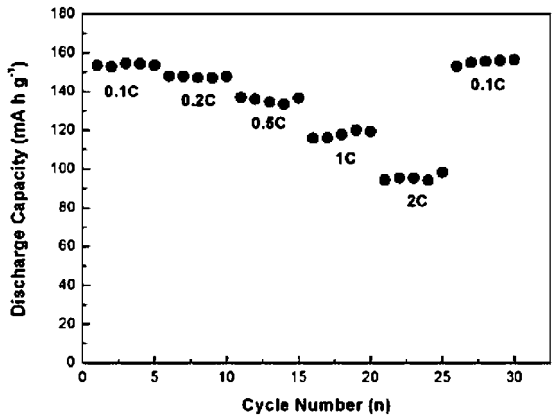

Fig. 7 Discharge capacity *vs.* cycle number at various discharge rates of $LiFePO_4$/C (sample (c)) synthesized with $scCO_2$.

It is well known that the property of $scCO_2$ strongly depends on the employed temperature and pressure, and thus might consequentially affect the performance of the synthesized material. In order to check the effect of reaction temperature on morphology and electrochemical properties of the $LiFePO_4$/C, four additional samples are prepared in $scCO_2$ at different temperatures (50, 100, 150 and 200 °C). As can be seen in Fig. 8, XRD patterns indicate that all the samples can also be indexed to the pure $LiFePO_4$ phase. The absence of the diffraction peaks for carbon coating is due to its low content and amorphous state.

The morphologies of these four $LiFePO_4$/C products are illustrated in Fig. 9. It is found that the particle size of the samples grows obviously as the reaction temperature increases. For example, the primary diameter grows from approximately 0.5 to 2 μm when the reaction temperature increases from 50 to 200 °C. In addition, the particle aggregation becomes especially serious for the samples prepared at 150 and 200 °C, where most of the small particles connected to big ones and their particle shapes are relatively irregular. This serious agglomeration of the particles would accordingly affect their electrochemical performance.

Fig. 10 shows the initial discharge profiles of $LiFePO_4$/C samples at 0.1 C rate. It is found that, when the reaction temperature increases from 50 to 200 °C, the initial discharge capacity decreases from 158 to 41 mA h g^{-1}, indicating that 50 °C

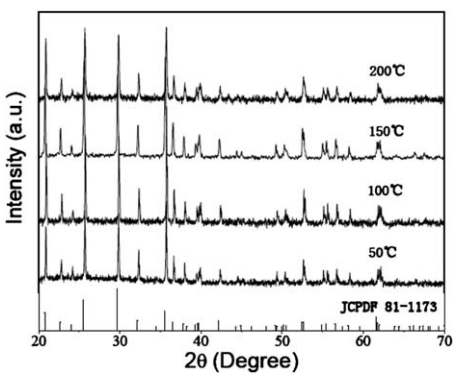

Fig. 8 XRD patterns of the samples synthesized with $scCO_2$ at different temperatures.

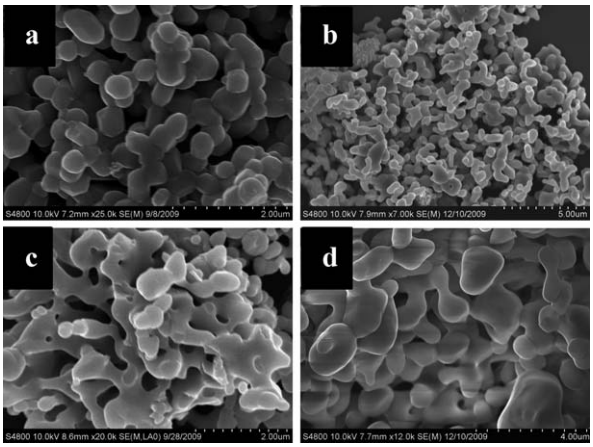

Fig. 9 SEM images of the samples synthesized with $scCO_2$ at different temperatures (a, 50 °C; b, 100 °C; c, 150 °C; d, 200 °C).

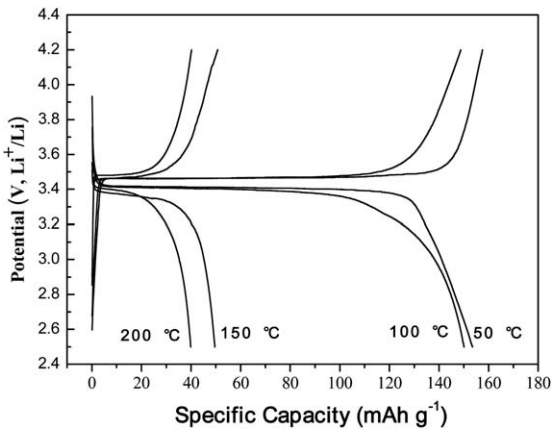

Fig. 10 The initial charge/discharge profiles of samples synthesized with $scCO_2$ at different temperatures.

Table 1 Carbon content and electronic conductivity of $LiFePO_4$/C powders synthesized in $scCO_2$ at different temperatures

Reaction temperature/°C	50	100	150	200
Carbon content (%)	5.3	5.1	2.2	2.1
Conductivity/S cm^{-1}	1.5×10^{-3}	5.6×10^{-4}	5.7×10^{-7}	2.1×10^{-7}

is the optimum temperature to synthesize $LiFePO_4$ in $scCO_2$ in our experiments. The poor electrochemical performance of $LiFePO_4$/C with a larger size prepared at elevated temperatures implies that the lithium-ion diffusion coefficient might be not favourable in these cases. On the other hand, the decrease in carbon content and conductivity (Table 1) of $LiFePO_4$/C samples at elevated temperatures is in good agreement with their electrochemical performance.

Conclusions

In this work, we describe a new synthesis method for carbon coated $LiFePO_4$ ($LiFePO_4$/C), wherein $scCO_2$ is used as a solvent and low-cost $Fe(NO_3)_3 \cdot 9H_2O$ as a precursor. The XRD and XPS confirm the success of synthesis of high purity $LiFePO_4$/C composite. The SEM images show that $scCO_2$ plays a crucial role in the morphology of $LiFePO_4$/C. The TEM and SAED results further reveal that the carbon coated particle is single-crystalline and can be indexed as the $LiFePO_4$ orthorhombic phase. As for the electrochemical performance, it is found that, at a current rate of 0.1 C, the discharge capacity of $LiFePO_4$/C synthesized in $scCO_2$ is 158 mA h g^{-1}, which is close to the theoretical capacity of 170 mA h g^{-1} and much higher than those containing $LiFePO_4$/C prepared in other solvents. Furthermore, this high discharge capacity can be retained up to 100 cycles. In order to check the effect of reaction temperature on the morphology and electrochemical properties of $LiFePO_4$/C, four additional samples are prepared in $scCO_2$ at different temperatures. Although the pure $LiFePO_4$ phase can be obtained in all cases, the primary particle size grows seriously and the initial discharge capacity decreases from 158 mA h g^{-1} to 41 mA h g^{-1} when the temperature increases from 50 to 200 °C, indicating that 50 °C is the optimum temperature to synthesize $LiFePO_4$. Note that after continuous efforts, some supercritical fluid applications are already at industrial capacity, whereas others remain under development. We hope our proposed method here could be used for large scale yield in industrial production in future.

Acknowledgements

This work was financially supported by the Foundation for Innovative Research Groups of the National Natural Science Foundation of China (No. 20921002) and by the analysis and testing foundation of Changchun Institute of Applied Chemistry.

References

1 J. Y. Kim and D. Y. Lim, *Energies*, 2010, **3**, 866.
2 F. Y. Cheng, Z. L. Tao, J. Liang and J. Chen, *Chem. Mater.*, 2008, **20**, 667.
3 M. S. Whittingham, *Chem. Rev.*, 2004, **104**, 4271.
4 A. K. Padhi, K. S. Nanjundaswamy and J. B. Goodenough, *J. Electrochem. Soc.*, 1997, **144**, 1188.
5 H. Yang, X. L. Wu, M. H. Cao and Y. G. Guo, *J. Phys. Chem. C*, 2009, **113**, 3345.
6 N. Recham, L. Dupont, M. Courty, K. Djellab, D. Larcher, M. Armand and J. M. Tarascon, *Chem. Mater.*, 2009, **21**, 1096.
7 Y. G. Wang, Y. R. Wang, E. Hosono, K. X. Wang and H. Zhou, *Angew. Chem., Int. Ed.*, 2008, **47**, 7461.
8 L. Wang, Y. D. Huang, R. R. Jiang and D. Z. Jia, *Electrochim. Acta*, 2007, **52**, 6778.
9 F. Gao, Z. Y. Tang and J. J. Xue, *Electrochim. Acta*, 2007, **53**, 1939.
10 A. V. Murugan, T. Muraliganth and A. Manthiram, *Electrochem. Commun.*, 2008, **10**, 903.
11 K. Kim, J. H. Jeong, I. J. Kim and H. S. Kim, *J. Power Sources*, 2007, **167**, 524.
12 S. Y. Chung, J. T. Bloking and Y. M. Chiang, *Nat. Mater.*, 2002, **1**, 123.
13 P. S. Herle, B. Ellis, N. Coombs and L. F. Nazar, *Nat. Mater.*, 2004, **3**, 147.
14 N. Ravet, Y. Chouinard, J. F. Magnan, S. Besner, M. Gauthier and M. Armand, *J. Power Sources*, 2001, **97–98**, 503.
15 H. Huang, S. C. Yin and L. F. Nazar, *Electrochem. Solid-State Lett.*, 2001, **4**, A170.
16 P. P. Prosini, D. Zane and M. Pasquali, *Electrochim. Acta*, 2001, **46**, 3517.
17 Y. S. Hu, Y. G. Guo, R. Dominko, M. Gaberscek, J. Maier and J. Jamnik, *Adv. Mater.*, 2007, **19**, 1963.
18 F. Croce, A. D. Epifanio, J. Hassoun, A. Deptula, T. Olczac and B. Scrosati, *Electrochem. Solid-State Lett.*, 2002, **5**, A47.

19 X. Li, W. Wang, C. Shi, H. Wang and Y. Xing, *J. Solid State Electrochem.*, 2009, **13**, 921.
20 K. S. Park, S. B. Schougaard and J. B. Goodenough, *Adv. Mater.*, 2007, **19**, 848.
21 R. Dominko, M. Bele, M. Gaberscek, M. Remskar, D. Hanzel, J. M. Goupil, S. Pejovnik and J. Jamnik, *J. Power Sources*, 2006, **153**, 274.
22 C. Delacourt, P. Poizot, S. Levasseur and C. Masquelier, *Electrochem. Solid-State Lett.*, 2006, **9**, A352.
23 J. Barker, M. Y. Saidi and J. L. Swoyer, *Electrochem. Solid-State Lett.*, 2003, **6**, A53.
24 C. Delmas, M. Maccario, L. Crogunnec, F. L. Cras and F. Weill, *Nat. Mater.*, 2008, **7**, 665.
25 B. Kang and G. Ceder, *Nature*, 2009, **458**, 190.
26 J. M. Tarascon, N. Recham, M. Armand, J. N. Chotard, P. Barpanda, W. Walker and L. Dupont, *Chem. Mater.*, 2010, **22**, 724.
27 T. Seki, J. D. Grunwaldt and A. Baiker, *Ind. Eng. Chem. Res.*, 2008, **47**, 4561.
28 Y. Q. Wang, J. L. Wang, J. Yang and Y. N. Niu, *Adv. Funct. Mater.*, 2006, **16**, 2135.
29 K. S. Tan, M. V. Reddy, G. V. Subba Rao and B. V. R. Chowdari, *J. Power Sources*, 2005, **141**, 129.
30 Y. H. Rho, L. F. Nazar, L. Perry and D. Ryan, *J. Electrochem. Soc.*, 2007, **154**, A283.
31 A. Caballero, M. C. Yusta, J. Morales, J. S. Pena and E. R. Castellon, *Eur. J. Inorg. Chem.*, 2006, 1758.
32 X. G. Peng, J. Wickham and A. P. Alivisatos, *J. Am. Chem. Soc.*, 1998, **120**, 5343.
33 H. T. Hsieh, W. K. Chin and C. S. Tan, *Langmuir*, 2010, **26**, 10031.
34 R. A. Lucky, R. H. Sui, J. M. H. Lo and P. A. Charpentier, *Cryst. Growth Des.*, 2010, **10**, 1598.

